J. Membrane Biol. 214, 131–138 (2006)
DOI: 10.1007/s00232-006-0051-0

The Journal of
Membrane
Biology

The Polarity of Lipid-Exposed Residues Contributes to the Functional Differences between *Torpedo* and Muscle-Type Nicotinic Receptors

Gisila R. Guzmán[1], Alejandro Ortiz-Acevedo[1], Ariamsi Ricardo[1], Legier V. Rojas[2], José A. Lasalde-Dominicci[1]
[1]Department of Biology, University of Puerto Rico, San Juan, Puerto Rico 00931-3360
[2]Department of Physiology, School of Medicine, Universidad Central del Caribe, Bayamón, Puerto Rico 00960-6032

Received: 29 June 2006/Revised: 27 November 2006

Abstract. A comparison between the *Torpedo* and muscle-type acetylcholine receptors (AChRs) reveals differences in several lipid-exposed amino acids, particularly in the polarity of those residues. The goal of this study was to characterize the role of eight lipid-exposed residues in the functional differences between the *Torpedo* and muscle-type AChRs. To this end, residues αS287, αC412, βY441, γM299, γS460, δM293, δS297 and δN305 in the *Torpedo* AChR were replaced with those found in the muscle-type receptor. Mutant receptor expression was measured in *Xenopus* oocytes using [^{125}I]-α-bungarotoxin, and AChR ion channel function was evaluated using the two-electrode voltage clamp. Eight mutant combinations resulted in an increase (1.5- to 5.2-fold) in AChR expression. Four mutant combinations produced a significant 46% decrease in the ACh 50% inhibitory concentration (EC_{50}), while three mutant combinations resulted in 1.7- to 2-fold increases in ACh EC_{50}. Finally, seven mutant combinations resulted in a decrease in normalized, ACh-induced currents. Our results suggest that these residues, although remote from the ion channel pore, (1) contribute to ion channel gating, (2) may affect trafficking of AChR into specialized membrane domains and (3) account for the functional differences between *Torpedo* and muscle-type AChR. These findings emphasize the importance of the lipid-protein interface in the functional differences between the *Torpedo* and muscle-type AChRs.

Key words: Acetylcholine receptor — Site-directed mutagenesis — *Xenopus* oocyte — Lipid-exposed residue — *Torpedo californica* — Muscle-type receptor

Correspondence to: José A. Lasalde-Dominicci; email: joseal@coqui.net

Introduction

The *Torpedo* acetylcholine receptor (AChR) is a pentamer with a subunit stoichiometric ratio of 2α:β:γ:δ. Each of these subunits has four transmembrane (TM) domains, M1–M4. TM1 and TM2 line the ion channel pore (Akabas & Karlin, 1995), while TM3 and TM4 are in contact with the membrane lipids (Blanton & Cohen, 1992, 1994; Blanton et al., 1998; Miyazawa, Fujiyoshi & Unwin, 2003) and thus constitute the AChR's lipid-protein interface. The amino acid similarity of the *Torpedo* AChR α-, β-, γ- and δ-subunits suggests a common ancestor for the genes encoding for these subunits (Noda et al., 1983).

Even though there is a high degree of sequence identity between the *Torpedo* and mouse (muscle-type) AChRs, these two subtypes exhibit different functional properties. Moreover, there are marked functional differences between fetal and adult muscle-type AChRs (Bouzat, Bren & Sine, 1994). For example, the muscle-type AChR expressed in *Xenopus* oocytes has a mean open time of 3.75 ms in the adult type (αβεδ) and 4.86 ms in the embryonic type (αβγδ), when using 4.0 μM ACh and a holding potential of –100 m*V* (Tamamizu et al., 1999). In contrast, using the same expression system and experimental conditions, the *Torpedo* AChR displays a mean open time one order of magnitude lower, 0.2–0.3 ms (Lee at al., 1994; Tamamizu et al., 2000).

The main electrophysiological difference between *Torpedo* and muscle-type AChRs is the open channel probability (P_{open}). The *Torpedo* AChR expressed in oocytes displayed a $P_{open} < 0.05$, as determined by burst-oriented analysis (Ortiz-Miranda et al., 1997). Consistent with this small P_{open}, the ACh-induced macroscopic currents of the *Torpedo* AChR display a fast decay time. In contrast, the muscle-type AChR expressed in oocytes displays a large P_{open} (> 0.75),

Table 1. Differences among the residues in the M3 and M4 TM domains of the *Torpedo* and muscle-type AchRs

	M3	M3 lipid-exposed	M4	M4 lipid-exposed
α	3/23 → 13%	1/2 → 50%	5/20 → 25%	1/6 → 17%
β	4/23 → 17%	1/3 → 33%	9/20 → 45%	2/5 → 40%
γ	10/23 → 43%	2/4 → 50%	10/20 → 50%	1/3 → 33%
δ	9/23 → 39%	4/5 → 80%	9/20 → 45%	1/4 → 25%
Total	26/92 → 32%	8/14 → 57%	33/80 → 41%	5/18 → 28%
Total differences in M3 and M4: 59/172 → 34%.				
Total differences in M3 and M4 at the lipid-protein interface: 13/32 → 41%.				

Total amount of residues differing in the M3 and M4 TM domains of the *Torpedo* and muscle-type AChRs. The second and fourth columns summarize the comparison between the lipid-exposed residues (Blanton & Cohen, 1992, 1994; Blanton et al., 1998) in the M3 and M4 TM domains for the *Torpedo* and muscle-type AChRs.

which is consistent with the slow decay time in the ACh-induced macroscopic currents. The ACh 50% inhibitory concentration (EC_{50}) for the *Torpedo* AChR is about 13–20 μM, whereas that for the muscle-type is approximately 50 μM. Finally, in oocytes the *Torpedo* AChR desensitizes faster than the muscle-type AChR. Therefore, in this study, we used macroscopic current parameters to assess the functional effects of these lipid-exposed mutations.

Results from studies using mouse-*Torpedo* hybrids suggest that the α- and δ-subunits are responsible for the longer mean open times seen in the mouse AChR (Yu et al., 1991). Mouse-*Torpedo* chimeric α-subunits expressed in *Xenopus* oocytes showed that the region near the ACh binding site might be responsible for differences in the open time between the mouse and *Torpedo* AChRs (Butler et al., 1997). Studies using site-directed mutagenesis at residues in the lipid-protein interface reveal marked functional differences between the *Torpedo* and muscle-type AChRs (Lee et al., 1994; Tamamizu et al., 1999; Navedo et al., 2004). For instance, the αC418G mutation in the *Torpedo* AChR results in functional AChRs (Ortiz-Miranda et al., 1997); however, the same mutation in the muscle-type receptor does not produce functional AChRs in oocytes (Tamamizu et al., 1999). An equivalent mutation of a lipid-exposed residue, I290W, produces a gain-in-function response in *Torpedo* yet results in a loss-in-function response in the muscle-type nAChR (Navedo et al., 2004; Guzman et al., 2003; Otero-Cruz et al., 2006). This difference in response exposes the importance of the lipid-protein interface in the differential modulation of activity in the AChR subtypes. In addition, these results suggest a difference in the interaction between lipid-exposed residues and the lipid environment for these receptor subtypes.

Hydrophobic photolabeling of TM3 and TM4 has been successfully used to identify some of the lipid-exposed residues of the AChR (Blanton & Cohen, 1994; Blanton et al., 1998). To further characterize the differences between the *Torpedo* and muscle-type AChRs, we compared the sequences of each of these receptor's lipid-protein interface. In each of the M3 and M4 TM domains, at least one of the residues identified as lipid-exposed is not homologous (Table 1). An amino acid sequence comparison between these receptor subtypes reveals that 13 of the 32 residues identified as lipid-exposed are different. Based on the lipid-exposed residues so far identified, we calculate a 41% difference between the lipid-protein interfaces of these two receptor subtypes (Table 1).

The amino acids of these two receptor types also differ in their chemical properties. The *Torpedo* AChR possesses many polar residues at its lipid-protein interface, while the muscle-type receptor has nonpolar residues at the same positions (Table 2). Eight lipid-exposed positions (Blanton & Cohen, 1994) in the TM3 and TM4 domains of the *Torpedo* AChR have uncharged polar side chains (αS287, αC412, βY441, γM299, γS460, δM293, δS297 and δN305), while the same residues in the muscle-type receptor are nonpolar amino acids (αA287, αG412, βW441, γV299, γI460, δL293, δV297 and δI305). These differences in the chemical properties of the lipid-exposed domains could be responsible for the adaptation of these receptors to different membrane environments and their marked functional differences.

In this study, we examined the contribution of the TM3 and TM4 domains to the functional differences between the *Torpedo* and muscle-type AChRs. To this end, we systematically replaced eight *Torpedo* AChR residues with their analogous residues in muscle-type, for both M3 and M4 in the *Torpedo* AChR. The two additional criteria used for side chain replacements in the present study were as follows: (1) the residue was previously shown to be exposed to the membrane lipids and (2) the replacement results in a considerable change in polarity. Our data suggest that these eight residues, although remote from the ion channel pore, contribute to channel gating and to the functional differences between these receptors. Until recently, channel-lining residues within the

Table 2. Amino acid sequences of the M3 and M4 TM domains of the AChR subunits

	M3	M4
Torpedo α	GKYMLFTM**I**FVI**S**SIIITV**V**VIN	ILL**C**VFML**IC**I**I**GT**VS**VFAG
Mouse α	GKYMLFTM**V**FV**I**A**S**IIITV**I**VIN	ILL**G**VFML**VC**L**I**GT**LA**VFAG
Torpedo β	I**R**YLMF**I**M**I**LV**A**FSVILSVVVLN	LFL**YV**F**F**V**IC**S**I**GT**FS**IFLD
Mouse β	I**K**YLMF**T**M**V**LV**T**FSVILSVVVLN	LFL**WT**F**I**V**F**T**S**VGT**L**V**I**FLD
Torpedo γ	**G**KYL**I**FV**M**F**VSM**LIV**M**N**C**V**I**VLN	CF**WIA**LLLF**S**IGT**LA**IFL**TG**
Mouse γ	**S**KYL**T**F**LM**VV**TI**LIVVN**S**VVVLN	CF**LAMLS**LF**IC**GT**AG**IFL**MA**
Torpedo δ	GK**YLM**F**IMS**LVT**GVIVNCGI**VLN	**SMFII**TPVM**V**LGT**IF**IF**VMG**
Mouse δ	GK**FLLFGMV**LVT**MVVVICV**IVLN	**CLFVV**TPVM**V**VGT**A**W**I**F**LQG**

Residues in bold represent amino acid differences among the receptor species. Residues highlighted in yellow are lipid-exposed (based on [^{125}I]-TID and [^{3}H]-diazofluorene labeling studies [Blanton & Cohen, 1992, 1994; Blanton et al., 1998]) amino acids that are not conserved among the species.

AChR's TM1 and TM2 have been considered to be the most critical players in channel gating. It is becoming gradually apparent that TM domains far from the channel pore, e.g., TM4, play an important role in AChR gating dynamics (Mitra, Bailey & Auerbach, 2004). More specifically, the results presented here and elsewhere (Bouzat et al., 1998) are making progressively more evident the critical role that lipid-exposed residues within TM3 and TM4 have in ion channel function.

Methods

Mutations of the *Torpedo* α-, β-, γ- and δ-Subunits

M3 and M4 mutants were prepared using the Quick Change Site-Directed Mutagenesis kit (Stratagene, La Jolla, CA). Mutagenic primers containing the desired codon replacement were synthesized by Life Technologies-GIBCO BRL (Gaithersburg, MD). These primers extended 11–13 bases on either side of the mismatched region. The polymerase chain reaction protocol included denaturation of the plasmid for 30 s at 95°C, primer annealing for 1 min at 55°C and extension for 12 min at 68°C. Subsequent to DNA amplification, the samples were digested for 1 h with 10 units of *Dpn*I endonuclease at 37°C. These samples were used to transform *Epicurian coli* XL1 supercompetent cells. The DNA was isolated, purified using the QIAprep Spin Miniprep Kit (Qiagen, Germantown, MD) and sequenced to ensure successful mutagenesis.

In Vitro RNA Transcript Synthesis and Expression in *Xenopus oocytes*

cDNA templates corresponding to the α-, β-, γ- and δ-subunits of *Torpedo* AChR were linearized and subjected to *in vitro* transcription with the SP6 mMESSAGE mMACHINE Kit (Ambion, Austin, TX). An equimolar mixture of mRNA of α-, β-, γ- and δ-subunits was microinjected into oocytes (total of 40 ng/oocyte) using a displacement injector (Drummond Instruments, Broomhall, PA). The injected oocytes were incubated at 19°C for 3 days in 0.5x Leibovitz's L-15 medium (GIBCO BRL) supplemented with 400 μg/ml bovine serum albumin, 119 mg/ml penicillin, 200 mg/ml streptomycin and 110 mg/ml pyruvic acid. The medium was replaced daily.

Voltage Clamp on *Xenopus* Oocytes

Oocytes were used for the experiments 3–4 days after mRNA injection. To this end, oocytes were transferred to a recording chamber and continuously perfused with MOR2 buffer (115 mM NaCl, 2.5 mM KCl, 1 mM Na_2HPO_4, 5 mM $MgCl_2$, 0.2 mM $CaCl_2$, 0.5 mM ethyleneglycoltetraacetic acid [EGTA] and 5 mM 4-(2-hydroxyethyl)-1-piperazineethanesulfonic acid [HEPES], pH 7.4) at a rate of 15 ml/min. All reagents used were obtained from Sigma-Aldrich (St. Louis, MO). A GeneClamp 500B Amplifier (Axon Instruments, Union City, CA) was used to measure agonist-induced currents (22°C) using two-electrode voltage clamp. Membrane currents were digitized using a DigiData 1200 interface (Axon Instruments) and filtered at 2 kHz during recording. A Pentium III-based computer was used to perform data acquisition using the Whole Cell program (version 2.3; kindly provided by Dr. J. Dempster, University of Strathclyde, UK). Dose-response curves were prepared from peak currents using six ACh concentrations (1, 3, 10, 30, 100 and 300 μM). The number of oocytes used for each dose-response curve ranged 8–15. Dose-response data were analyzed using Prism 3.0 (Graphpad Software, San Diego, CA). A nonlinear regression fit was performed using the equation $I = I_{\min} + \left(I_{\max} - I_{\min}/I + 10^{(Log\,EC_{50} \cdot Log[ACh]) \times Hill\,Slope}\right)$. In this equation I is the macroscopic current at a given ACh concentration, $I_{\min}$ and $I_{\max}$ are the smallest and the largest currency observed, respectively, EC_{50} is the concentration required to achieve half-maximal response, and the Hill Slope is the slope of the linear portion of the sigmoidal curve. The EC_{50} and Hill coefficient values from individual oocytes were averaged, and statistical analysis was performed using Student's *t*-test (GraphPad Prism 3.0).

[^{125}I]-α-Bungarotoxin Binding Assay

We performed [^{125}I]α-bungarotoxin (Perkin-Elmer, Boston, MA) binding assays to determine the membrane expression of AChR in oocytes. The oocytes were incubated in 10 nM [^{125}I]α-bungarotoxin with 5 mg/ml bovine serum albumin in MOR-2 without EGTA (115 mM NaCl, 2.5 mM KCl, 5 mM $MgCl_2$, 1 mM Na_2HPO_4, 5 mM HEPES, 0.2 mM $CaCl_2$, pH 7.4) at room temperature for 1.5 h. Noninjected oocytes were also incubated in [^{125}I]α-bungarotoxin to measure nonspecific toxin binding (Beckman Gamma 5500; Beckman, Fullerton, CA). Excess toxin was removed by washing each oocyte with 15 ml of MOR-2 without EGTA. A standard curve was obtained by plotting the counts per minute against [^{125}I]α-bungarotoxin concentration (0.5–20 fmol). The equation for the linear regression obtained from this graph was used to calculate the AChR expression (fmol) present in the membrane of each oocyte.

Table 3. Functional consequences of lipid-exposed mutants

AChR type	Fmol	EC_{50} (μM ACh)	Hill coefficient	Normalized response (nA/fmol)	*n*
Torpedo αβγδ	2.1 ± 0.2	13 ± 3	1.6 ± 0.1	5,115 ± 171	9
Muscle-type αβϵδ	2.1 ± 0.5	54 ± 1	1.4 ± 0.5	722 ± 171	10
$\alpha_m\beta\gamma\delta$	2.6 ± 0.3	19 ± 4	1.4 ± 0.1	5,113 ± 659	10
$\alpha\beta_m\gamma\delta$	3.2 ± 0.3**	7 ± 1*	1.3 ± 0.2	4,390 ± 529	9
$\alpha\beta\gamma_m\delta$	2.1 ± 0.2	7 ± 1*	1.8 ± 0.1	4,324 ± 474	11
$\alpha\beta\gamma\delta_m$	2.4 ± 0.5	26 ± 4**	1.6 ± 0.1	3,263 ± 1,002	12
$\alpha\beta_m\gamma_m\delta_m$	11 ± 2*	22 ± 2*	1.6 ± 0.1	567 ± 101***	4
$\alpha_m\beta\gamma_m\delta_m$	6.1 ± 1.5	8 ± 5	1.4 ± 0.5	2,609 ± 922*	5
$\alpha_m\beta_m\gamma\delta_m$	6.7 ± 1.0**	9 ± 1	1.8 ± 0.2	1,041 ± 156***	5
$\alpha_m\beta_m\gamma_m\delta$	4.2 ± 0.8*	24 ± 4*	1.31 ± 0.06	2,093 ± 313***	5
$\alpha\beta\gamma_m\delta_m$	2.4 ± 1.0	15 ± 3	1.8 ± 0.4	8,066 ± 3,678	7
$\alpha\beta_m\gamma\delta_m$	4.1 ± 0.2***	14 ± 3	1.3 ± 0.1	3,409 ± 283*	6
$\alpha\beta_m\gamma_m\delta$	2.3 ± 0.4	12 ± 6	1.8 ± 0.3	3,661 ± 718	6
$\alpha_m\beta\gamma\delta_m$	3.6 ± 0.3**	7 ± 1*	1.9 ± 0.3	2,771 ± 341**	7
$\alpha_m\beta\gamma_m\delta$	4.2 ± 0.9	11 ± 2	1.9 ± 0.2	3,828 ± 1,954	6
$\alpha_m\beta_m\gamma\delta$	3.7 ± 0.4*	16 ± 2	1.58 ± 0.04	2,284 ± 168***	6
$\alpha_m\beta_m\gamma_m\delta_m$	6.1 ± 0.4***	7 ± 1*	2.1 ± 0.2*	3,363 ± 738	10

α_m = αS287A/C412G, β_m = βY441W, γ_m = γM299V/S460I, δ_m = δM293L/S297V/N305I. Values are given as the mean ± standard error. Normalized peak channel activity for individual oocytes was obtained by dividing the ACh-induced current at 300 μM by the fmol of AChR expressed on each oocyte.
*$P < 0.01$, **$P < 0.05$, ***$P < 0.001$.

The nAChR expression value for each oocyte was used to calculate the normalized channel response to ACh for each oocyte, which is defined as the ACh-induced current in nanoamperes divided by femtomoles of surface α-bungarotoxin binding. Student's *t*-test (GraphPad Prism 3.0) was used to determine statistical significance.

Results

Expression of AChR Mutants

Site-directed mutagenesis was performed at positions αS287/C412, βY441, γM299/S460 and δM293/S297/N305 of the *Torpedo* AChR. We prepared a single mutant in the β-subunit (βY441W [β_m]), a double mutant in the α– and γ–subunits (αS287A/C412G [α_m], γM299V/S460I [γ_m]) and a triple mutation in the δ–subunit (δM293L/S297V/N305I [δ_m]). A total of 15 mutant combinations were tested as they accounted for all of the possible combinations of these mutants.

The expression levels of each mutant combination, measured by [^{125}I]α-bungarotoxin binding, are summarized in Table 3. Eight of the mutant combinations resulted in expression more than twofold that of wild type. The most dramatic increase was observed in combination 5 (Table 3, $\alpha\beta_m\gamma_m\delta_m$), which resulted in a 5.5-fold increase in toxin binding (11 ± 2 fmol). Combinations 7 and 15 (Table 3, $\alpha_m\beta_m\gamma\delta_m$ and $\alpha_m\beta_m\gamma_m\delta_m$) resulted in a threefold increase in toxin binding (6.7 ± 1.0 and 6.1 ± 0.4). Finally, combinations 8 and 10 (Table 3, $\alpha_m\beta_m\gamma_m\delta$ and $\alpha\beta_m\gamma\delta_m$) resulted in a twofold increase in binding (4.2 ± 0.8 and 4.1 ± 0.2). None of the mutations studied decreased toxin binding. These results suggest that these eight mutated residues are important for the assembly of the AChR in the membrane.

Electrophysiological Analysis

Current traces for wild-type and all mutant combinations are shown in Figure 1. The data obtained from two-electrode voltage clamp were used to generate ACh dose-response curves for wild-type and all mutant combinations. The ACh concentrations used ranged 1–300 μM, as shown in Figure 1. Combinations 2, 3, 12 and 15 (Table 3, $\alpha\beta_m\gamma\delta$, $\alpha\beta\gamma_m\delta$, $\alpha_m\beta\gamma\delta_m$ and $\alpha_m\beta_m\gamma_m\delta_m$) resulted in a significant decrease in the ACh EC_{50}, with percent inhibition averaging 46%. In contrast, combinations 4, 5 and 8 (Table 3, $\alpha\beta\gamma\delta_m$, $\alpha\beta_m\gamma_m\delta_m$ and $\alpha_m\beta_m\gamma_m\delta$) increased the ACh EC_{50} by an average of 1.8-fold. Finally, mutant combinations 5, 6, 7, 8, 10, 12 and 14 (Table 3, $\alpha\beta_m\gamma_m\delta_m$, $\alpha_m\beta\gamma_m\delta_m$, $\alpha_m\beta_m\gamma\delta_m$, $\alpha_m\beta_m\gamma_m\delta$, $\alpha\beta_m\gamma\delta_m$, $\alpha_m\beta\gamma\delta_m$ and $\alpha_m\beta_m\gamma\delta$) resulted in normalized currents significantly lower than *Torpedo* wild type.

Discussion

Torpedo and muscle AChR subtypes show marked differences in their electrophysiological properties. The TM domains of the AChR, particularly the lipid-exposed residues within the TM domains, play an important role in this ligand-gated channel's function (Cruz-Martin et al., 2001; Guzman et al., 2003; Lasalde et al., 1996; Santiago et al., 2001; Wang et al., 1999; Bouzat et al., 1998). Many lipid-exposed resi-

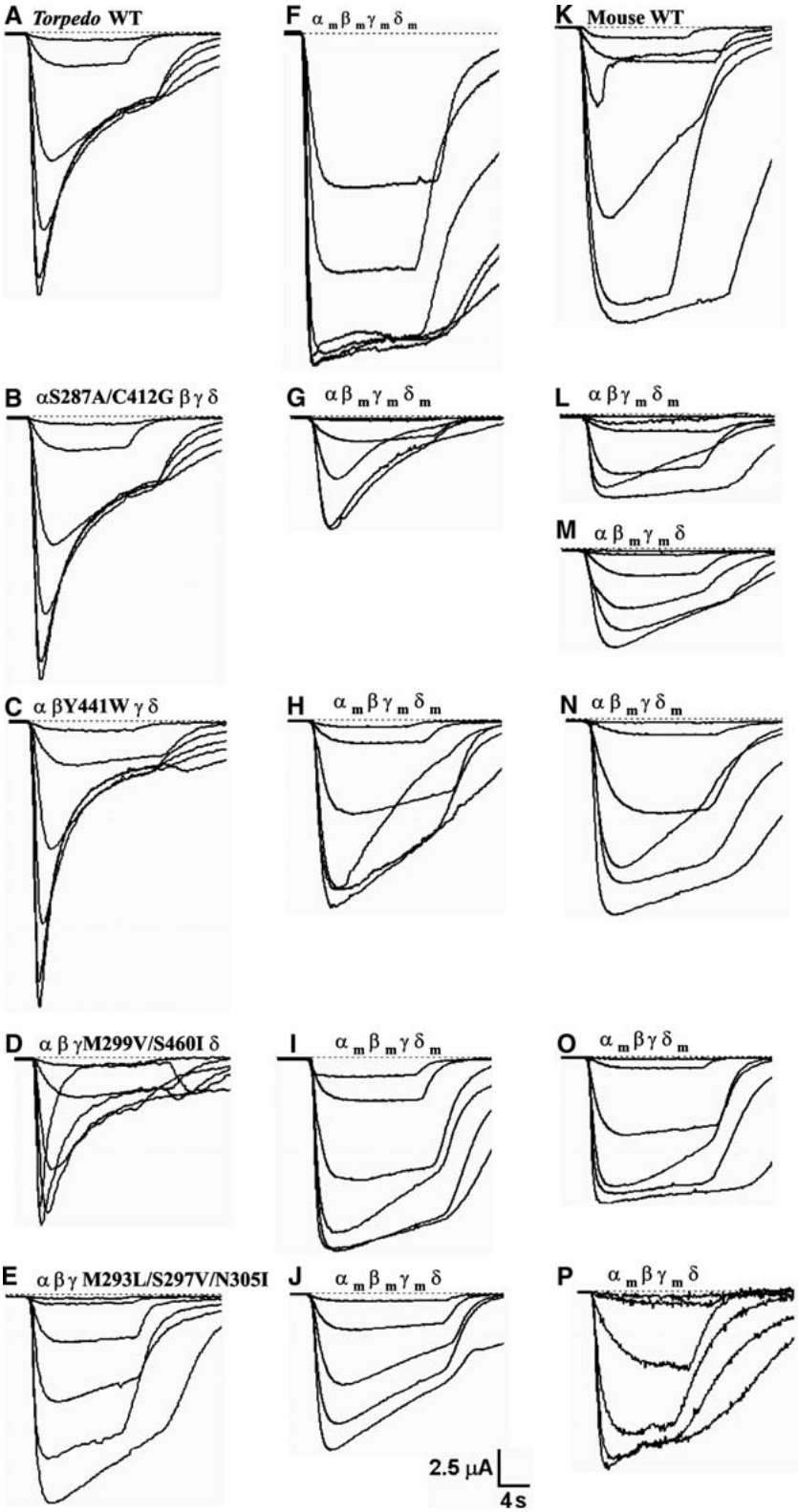

Fig. 1. Macroscopic current traces of wild-type and lipid-exposed mutant combinations. Macroscopic currents derived from individual oocytes expressing either wild-type or the various mutant combinations including αS287A/C412G (α_m), βY441W (β_m), γM299V/S460I (γ_m) and δM293L/S297V/N305I (δ_m). The currents were recorded using two-electrode voltage clamp. ACh-induced currents were detected at a membrane potential of –70 m*V* and filtered at 2 kHz. The ACh concentrations used to generate the family of currents were 1, 3, 10, 30, 100 and 300 μM. Representative current traces are shown from (*A*) *Torpedo* wild type, (*B*) αS287A/C412G, (*C*) βY441W, (*D*) γM299V/S460I, (*E*) M293L/S297V/N305I, (F) $\alpha_m\beta_m\gamma_m\delta_m$, (*G*) $\alpha\beta_m\gamma_m\delta_m$, (*H*) $\alpha_m\beta\gamma_m\delta_m$, (*I*) $\alpha_m\beta_m\gamma\delta_m$, (*J*) $\alpha_m\beta_m\gamma_m\delta$, (*K*) mouse wild type, (*L*) $\alpha\beta\gamma_m\delta_m$, (*M*) $\alpha\beta_m\gamma_m\delta$, (*N*) $\alpha\beta_m\gamma\delta_m$, (*O*) $\alpha_m\beta\gamma\delta_m$, (*P*) $\alpha_m\beta\gamma_m\delta$.

dues in the TM domains of the *Torpedo* AChR differ from those in the muscle-type AChR (Table 2). In addition, results from our previous studies suggest a marked difference in the interaction between lipid-exposed residues and the lipid environment for these receptor subtypes. In this study, we systematically replaced the lipid-exposed residues in the *Torpedo* AChR (Table 2, αS287/C412, βY441, γM299/S460

and δM293/S297/N305) with their analogous residues in the muscle-type AChR. This approach allowed us to determine the role of each of these residues in muscle-type AChR gating. A total of 15 possible combinations of these mutant subunits were generated, expressed in *Xenopus laevis* oocytes, and the expression levels of the mutants were estimated by [^{125}I]-α-bungarotoxin binding assays. Macroscopic ACh-induced currents were assessed using two-electrode voltage clamp.

The results from binding assays demonstrated that none of the mutations resulted in a decrease in AChR expression when compared to *Torpedo* wild type. In fact, eight of the 15 mutations resulted in a significant increase in expression (Table 3, combinations 2, 5, 7, 8, 10, 12, 14 and 15). It is noteworthy that the net effect of all of these substitutions is an increase in amino acid volume by 102 Å^3. Using the amino acid volumes reported by Chothia (1975), we calculated that in the α-subunit the net change in amino acid volume corresponds to a decrease by 46.8 Å^3, in the β-subunit a net increase by 34.6 Å^3, in the γ-subunit a net increase by 40.6 Å^3 and in the δ-subunit an increase by 73.3 Å^3. These data indicate that the *Torpedo* M3 and M4 domains tolerate the side chain increase of their homologous positions in the muscle-type.

ombination $\alpha\beta_m\gamma_m\delta_m$ (Table 3, combination 5) exhibited the most dramatic increase in AChR expression, thus suggesting that positions βY441, γM299, γS460, δM293, δS297 and δN305 of the muscle-type are involved in the efficiency of channel assembly and/or oligomerization. Interestingly, the substitutions in this combination result in a net increase in amino acid volume by 148 Å^3, the largest amino acid volume increase in all the mutant combinations. Combination 5 (Table 3), however, resulted in the largest decrease in function, as seen by a 1.7-fold increase in EC_{50} and an 89% decrease in normalized response (Table 3). Taken together, these data indicate that replacing lipid-exposed residues in *Torpedo* M3 and M4 domains with their analogues in the muscle-type AChR, which are nonpolar and have considerably bigger R groups, may help stabilize the AChR structure yet negatively affects channel function.

Combinations 2, 3, 12 and 15 (Table 3, $\alpha\beta_m\gamma\delta$, $\alpha\beta\gamma_m\delta$, $\alpha_m\beta\gamma\delta_m$ and $\alpha_m\beta_m\gamma_m\delta_m$) all resulted in a decrease in the EC_{50} for ACh. These results suggest that all the positions mutated in this study (αS287, αC412, βY441, γM299, γS460, δM293, δS297 and δN305) play a significant role in the AChR gating mechanism. It is possible that these *Torpedo* mutant combinations facilitated the conformational changes required for channel gating. These residues can be added to an exclusive group of lipid-exposed residues which, in response to hydrophobic substitutions, result in a gain in function. The aforementioned group includes the αF284 (Guzmán et al., 2003), αC418 (Lee et al., 1994), βC447 (Lasalde et al., 1996), αV425 (Tamamizu et al., 2000), γF292 and γL296 (Cruz-Martin et al., 2001) residues.

Our results also suggest that the lipid-exposed residues in the TM domains are responsible for the functional differences between these receptors. This is clearly evident from the results obtained with the *Torpedo* mutant combination which most closely resembles the muscle-type receptor, combination 15 (Table 3, $\alpha_m\beta_m\gamma_m\delta_m$). Specifically, Figure 1 illustrates that the ACh-induced macroscopic currents observed in combination 15 (Fig. 1F) resemble more those observed in the muscle-type receptor (Fig. 1K) than those observed in *Torpedo* wild-type currents (Fig. 1A). It could be argued that, in terms of EC_{50}, combination 15 resembles more the *Torpedo* than the muscle-type receptor (*see* Table 3). The muscle-type receptor contains the ϵ-subunit, which causes the receptor to have a decreased P_{open} (Naranjo & Brehm, 1993). The absence of ϵ in combination 15 could be an important factor influencing its EC_{50}.

The overall structure of the *Torpedo* AChR has been recently determined (Miyazawa et al., 2003; Unwin, 2005) using cryomicroscopy. This structure, which is solely based on the closed channel state, suggests that all TM domains are helical. In this study, we compared both muscle-type and *Torpedo* AChRs. The replacements made at the lipid-protein interface of the *Torpedo* receptor with the nonpolar amino acid side chains of the muscle-type AChR may result in localized structural alterations, which will in turn alter channel function (Otero-Cruz et al., 2006). For instance, some of the residues mutated (αS287, βY441, γS460, δS297 and δN305) might be interrupting hydrogen bonds or disulfide bridges formed by αC412, yet favoring the formation of van der Waals or dipole interactions, which can stabilize the protein by hydrophobic interactions.

All of the mutant combinations used in this study resulted in normal nAChR expression levels, thus demonstrating no problem in nAChR assembly and/or oligomerization. The normalized currents (nA/fmol) presented in Table 3 may give the impression that some mutations resulted in oligomerization problems. That is, when compared to *Torpedo* wild type, some mutations resulted in lower normalized currents. A possible explanation for these observations is that a single point mutation at the lipid interface alters trafficking of AChRs into specialized membrane domains. These lipid-exposed mutants may be preferentially located in caveolae because the mutations introduce a caveolin-binding motif (Couet et al., 1997). Although α-bungarotoxin labels AChRs which are localized in the caveolar domains, these receptors are presumably trapped in a nonconductive state. This would result in the estimation of an apparent reduction in the normalized current. We anticipated the existence of these reservoirs of

receptors in previous studies (Santiago et al., 2001; Tamamizu et al., 2000).

In the present study, this situation is more evident in mutations (and combinations of mutations) involving β_m (βY441W). In this case, by virtue of the fact that a tyrosine (polar aromatic) is being replaced with tryptophan (nonpolar aromatic), a stronger caveolin-binding motif is introduced with β_m (Couet et al., 1997). The data summarized in Table 3 show that even though combinations 5, 7, 8, 12 and 14 (all including β_m) result in normal expression, the normalized ACh-induced currents are lower than wild type. It is thus very likely that some of the mutations, particularly those including β_m, unexpectedly induced the preferential transport of these AChRs into cholesterol-rich domains (caveolae) within the oocyte membrane. Within these caveolae, the AChRs would be accessible to α-bungarotoxin labeling, yet a large fraction of these receptors would be nonconductive (Santiago et al., 2001).

An emerging hypothesis is that these nonpolar amino acids maximize the association energy with the lipid bilayer, consequently altering channel gating. A different interpretation is that the polar groups of the lipid-exposed residues of the *Torpedo* receptor are involved in the stabilization of unique interactions with other subunits or with the lipid interface, leading to different adaptations to the lipid environment.

In conclusion, electrophysiological analysis of the mutations in the M3 and M4 TM domains showed the role of the lipid-protein interface in the ion channel function of the AChR. The present study confirms that the TM3 and TM4 of all the subunits are critical to the kinetic properties of the AChR. These results indicate the importance of the lipid-protein interface to the AChR adaptation to different membrane environments.

This work was supported in part by grants from the National Institutes of Health: 2RO1GM5637-10 and GM08102-27, as well as UPR Institutional Funds for Research awarded to J.A. Lasalde-Dominicci. G. Guzman was supported by NSF-AGEP grant HRD-9817642 and A. Ricardo by NIH-MARC grant 5T34GM07821.

References

Akabas, M.H., Karlin, A. 1995. Identification of acetylcholine receptor channel-lining residues in the M1 segment of the alpha-subunit. *Biochemistry* **34:**12496–12500

Blanton, M.P., Cohen, J.B. 1992. Mapping the lipid-exposed regions in the *Torpedo californica* nicotinic acetylcholine receptor. *Biochemistry* **31:**3738–3750Erratum in *Biochemistry* 31:5951

Blanton, M.P., Cohen, J.B. 1994. Identifying the lipid-protein interface of the *Torpedo* nicotinic acetylcholine receptor: Secondary structure implications. *Biochemistry* **33:**2859–2872

Blanton, M.P., Dangott, L.J., Raja, S.K., Lala, A.K., Cohen, J.B. 1998. Probing the structure of the nicotinic acetylcholine receptor ion channel with the uncharged photoactivable compound ^{3}H-diazofluorene. *J. Biol. Chem.* **273:** 8659–8668

Bouzat, C., Bren, N., Sine, S.M. 1994. Structural basis of the different gating kinetics of fetal and adult acetylcholine receptors. *Neuron* **13:**1395–1402

Bouzat, C., Roccamo, A.M., Garbus., I., Barrantes, F.J. 1998. Mutations at lipid-exposed residues of the acetylcholine receptor affect its gating kinetics. *Mol. Pharmacol.* **54:**146–153

Butler, D.H., Lasalde, J.A., Butler, J.K., Tamamizu, S., Zimmerman, G., McNamee, M.G. 1997. Mouse-*Torpedo* chimeric alpha-subunit used to probe channel-gating determinants on the nicotinic acetylcholine receptor primary sequence. *Cell. Mol. Neurobiol.* **17:**13–33

Chothia, C. 1975. Structural invariants in protein folding. *Nature* **254:**304–308

Couet, J., Li, S., Okamoto, T., Ikezu, T., Lisanti, M.P. 1997. Identification of peptide and protein ligands for the caveolin-scaffolding domain. Implications for the interaction of caveolin with caveolae-associated proteins. *J. Biol. Chem.* **272:**6525–6533

Cruz-Martin, A., Mercado, J.L., Rojas, L.V., McNamee, M.G., Lasalde-Dominicci, J.A. 2001. Tryptophan substitutions at lipid-exposed positions of the gamma M3 transmembrane domain increase the macroscopic ionic current response of the *Torpedo californica* nicotinic acetylcholine receptor. *J. Membr. Biol.* **183:**61–70

Guzman, G.R., Santiago, J., Ricardo, A., Marti-Arbona, R., Rojas, L.V., Lasalde-Dominicci, J.A. 2003. Tryptophan scanning mutagenesis in the alpha M3 transmembrane domain of the *Torpedo californica* acetylcholine receptor: Functional and structural implications. *Biochemistry* **42:**12243–12250

Lasalde, J.A., Tamamizu, S., Butler, D.H., Vibat, C.R., Hung, B., McNamee, M.G. 1996. Tryptophan substitutions at the lipid-exposed transmembrane segment M4 of *Torpedo californica* acetylcholine receptor govern channel gating. *Biochemistry* :14139–14148

Lee, Y.H., Li, L., Lasalde, J., Rojas, L., McNamee, M., Ortiz-Miranda, S.I., Pappone, P. 1994. Mutations in the M4 domain of *Torpedo californica* acetylcholine receptor dramatically alter ion channel function. *Biophys. J.* **66:**646–653

Miyazawa, A., Fujiyoshi, Y., Unwin, N. 2003. Structure and gating mechanism of the acetylcholine receptor pore. *Nature* **423:**949–955

Naranjo, D., Brehm, P. 1993. Modal shifts in acetylcholine receptor channel gating confer subunit-dependent desensitization. *Science* **260:**1811–1814

Navedo, M., Nieves, M., Rojas, L., Lasalde-Dominicci, J.A. 2004. Tryptophan substitutions reveal the role of nicotinic acetylcholine receptor alpha-TM3 domain in channel gating: differences between *Torpedo* and muscle-type AChR. *Biochemistry* **43:**78–84

Noda, M., Takahashi, H., Tanabe, T., Toyosato, M., Kikyotani, S., Furutani, Y., Hirose, T., Takashima, H., Inayama, S., Miyata, T., Numa, S. 1983. Structural homology of *Torpedo californica* acetylcholine receptor subunits. *Nature* **302:**528–532

Mitra, A., Bailey, T.D., Auerbach, A.L. 2004. Structural dynamics of the M4 transmembrane segment during acetylcholine receptor gating. *Structure* **12:**1909–1918

Ortiz-Miranda, S.I., Lasalde, J.A., Pappone, P.A., McNamee, M.G. 1997. Mutations in the M4 domain of the *Torpedo californica* nicotinic acetylcholine receptor alter channel opening and closing. *J. Membr. Biol.* **158:**17–30

Otero-Cruz, J.D., Báez-Pagán, C.A., Caraballo-González, I.M., Lasalde-Dominicci, J.A. 2007. Tryptophan-scanning Muta-

genesis in the αM3 Transmembrane Domine of the Muscle-type Acetylcholine Receptor: A SPRING MODEL REVEALED. J. Biol. Chem. 282:9162–9171

Santiago, J., Guzman, G.R., Rojas, L.V., Marti, R., Asmar-Rovira, G.A., Santana, L.F., McNamee, M., Lasalde-Dominicci, J.A. 2001. Probing the effects of membrane cholesterol in the *Torpedo californica* acetylcholine receptor and the novel lipid-exposed mutation alpha C418W in *Xenopus* oocytes. *J. Biol. Chem.* **276:**46523–46532

Tamamizu, S., Lee, Y., Hung, B., McNamee, M.G., Lasalde-Dominicci, J.A. 1999. Alteration in ion channel function of mouse nicotinic acetylcholine receptor by mutations in the M4 transmembrane domain. *J. Membr. Biol.* **170:**157–164Erratum in *J. Membr. Biol.* 1999;172:89

Tamamizu, S., Guzman, G.R., Santiago, J., Rojas, L.V., McNamee, M.G., Lasalde-Dominicci, J.A. 2000. Functional effects of periodic tryptophan substitutions in the alpha M4 transmembrane domain of the *Torpedo californica* nicotinic acetylcholine receptor. *Biochemistry* **39:**4666–4673

Unwin, N. 2005. Refined structure of the nicotinic acetylcholine receptor at 4Å resolution. *J. Mol. Biol.* **346:**967–989

Wang, H.L., Milone, M., Ohno, K., Shen, X.M., Tsujino, A., Batocchi, A.P., Tonali, P., Brengman, J., Engel, A.G., Sine, S.M. 1999. Acetylcholine receptor M3 domain: Stereochemical and volume contributions to channel gating. *Nat. Neurosci.* **2:**226–233Erratum in *Nat. Neurosci.* 1999;2:485

Yu, L., Leonard, R.J., Davidson, N., Lester, H.A. 1991. Single-channel properties of mouse-*Torpedo* acetylcholine receptor hybrids expressed in *Xenopus* oocytes. *Brain Res. Mol. Brain Res.* :203–211